Published in final edited form as:
Neuron. 2013 August 7; 79(3): 447–460. doi:10.1016/j.neuron.2013.05.035.

Activity-induced convergence of APP and BACE-1 in acidic microdomains via an endocytosis-dependent pathway

Utpal Das[1,2], **David Scott**[1,2], **Archan Ganguly**[1,2], **Edward H. Koo**[2], **Yong Tang**[1,2], and **Subhojit Roy**[1,2,*]

[1]Department of Pathology, University of California, San Diego, 9500 Gilman Drive, La Jolla, CA 92093, USA

[2]Department of Neurosciences, University of California, San Diego, 9500 Gilman Drive, La Jolla, CA 92093, USA

Abstract

The convergence of APP (substrate) and BACE-1 (enzyme) is a rate-limiting, obligatory event triggering the amyloidogenic pathway – a key step in Alzheimer's disease (AD) pathology. However, as both APP/BACE-1 are highly expressed in brain, mechanisms precluding their unabated convergence are unclear. Exploring dynamic localization of APP/BACE-1 in cultured hippocampal neurons, we found that after synthesis via the secretory-pathway, dendritic APP/BACE-1-containing vesicles are largely segregated in physiologic states. While BACE-1 is largely sorted into acidic recycling endosomes, APP is conveyed in Golgi-derived vesicles. However upon activity-induction – a known trigger of the amyloidogenic pathway – APP is routed into BACE-1-positive recycling endosomes via a clathrin-dependent mechanism. A partitioning/convergence of APP/BACE-1 vesicles is also apparent in control/AD brains respectively. Considering BACE-1 is optimally active in an acidic environment, our experiments suggest that neurons have evolved trafficking strategies that normally limit APP/BACE-1 proximity; and also uncover a pathway routing APP into BACE-1-containing organelles – triggering amyloidogenesis.

Keywords

amyloid precursor protein (APP); β-site APP cleaving enzyme (BACE-1); vesicle trafficking; neuronal activity; recycling endosomes

INTRODUCTION

The amyloid precursor protein (APP) is sequentially cleaved to generate amyloid-beta (Aβ) peptides – pathologic hallmarks of AD – via the 'amyloidogenic pathway'. The rate-limiting step in this pathway is the cleavage of APP by the aspartyl protease β-site APP-cleaving enzyme-1 (BACE-1); making the physical proximity of APP (substrate) and BACE-1 (enzyme) an obligatory step initiating this pathway (Thinakaran and Koo, 2008). As continued proximity of APP/BACE-1 might lead to relentless pathology, it seems reasonable that cellular pathways would spatially segregate this enzyme/substrate pair in physiologic

*Corresponding author: Subhojit Roy, MD, PhD, 9500 Gilman Drive, BSB 1030A, MC0612, University of California, San Diego, CA 92093, USA, Telephone: 858-822-0125, s1roy@ucsd.edu.

states. However, to date the precise trafficking pathways of APP and BACE-1 in neurons – including mechanisms that dictate divergence/convergence of these two proteins – are unclear.

While previous studies have examined the sub-cellular localization of the trans-membrane proteins APP and BACE-1, there are two major caveats. First, most studies have been performed in a variety of non-neuronal cells or neuronal cell-lines that lack the unique morphology/compartmentalization of neurons. Accordingly, reported locales of these proteins range from the endoplasmic-reticulum (ER)/Golgi, cell membranes/lipid rafts, to endosomal-lysosomal organelles (Greenfield et al., 1999; Ehehalt et al., 2003 - reviewed in Brunholz et al., 2011 and Rajendran and Annaert, 2012). Furthermore, most have examined the trafficking of mutant (and not wild-type) APP. Secondly, the vast majority of studies have been performed in fixed cells, and have not fully accounted for the dynamic nature of these peptides, that are continuously trafficking in neurons (see below). Importantly, vesicle-trafficking pathways in highly polarized cells like neurons are unique compared to other cell-types. For instance neurons have an extensive and sophisticated network of recycling endosomes that are scattered throughout the processes, unlike non-neuronal cells where this system is relatively small and typically clustered around the nucleus (Yap and Winckler, 2012). Although some studies have examined APP/BACE-1 in polarized epithelial cells, extrapolation of these data to neurons has been complicated – reviewed in Haass et al., 2012.

Towards this we explored the dynamic localization of APP and BACE-1 in cultured hippocampal neurons, expressing low levels of fluorescent-tagged proteins and examining their trafficking and organelle-composition in neuronal soma and processes by high-resolution. We also designed imaging paradigms that revealed basic mechanisms leading to APP/BACE-1 convergence and initiation of the amyloidogenic pathway. Finally, we also examined the spatial localization of these proteins in mouse and human brains *in-vivo*. Our data reveal surprising aspects of APP/BACE-1 trafficking that were previously unknown, and help define a mechanistic pathway for activity-dependent amyloidogenesis.

RESULTS

Segregation of APP and BACE-1 into distinct neuronal microdomains

We first visualized the trafficking of APP and BACE-1 in neurons. Towards this we transfected cultured hippocampal neurons with low levels of APP/BACE-1 tagged to green/red fluorescent proteins (GFP/mCherry, see Supplementary fig. 1A–D), and simultaneously visualized their trafficking in somato-dendritic compartments after 4–6 hours – a time when these fusion proteins are just starting to be expressed (schematic in fig. 1A). We focused on somato-dendritic compartments as the spatial separation/convergence of APP/BACE-1 fluorescence could be confidently evaluated in these wider profiles (see below); recent reports also implicate dendrites in APP processing (Wei et al., 2010; Wu et al., 2012). Tubulo-vesicular structures carrying APP and BACE-1 moved bi-directionally within the dendritic shaft and the movement was microtubule-dependent, resembling the movement of motor-driven vesicular cargoes (Supplementary fig. 1E, F; Supplementary Movie 1; Supplementary Table and also see Tang et al. 2012). As shown in the kymographs (fig. 1B), localization of both stationary and mobile APP/BACE-1 particles were largely non-overlapping (fig. 1B, bar-graph). Subtle differences were also seen in the transport kinetics of APP and BACE-1 vesicles (fig. 1C), further suggesting that these two cargoes were largely conveyed in distinct organelles.

Next, to examine the biogenesis of APP/BACE-1 cargoes, we focused on the distribution of these proteins within the neuronal soma. As both APP and BACE-1 are trans-membrane proteins, they would be expected to traffic via the ER→Golgi (biosynthetic) pathway. In

accordance with this, we found significant colocalization of APP and BACE-1 in the perinuclear region (fig. 1D) – a distribution reminiscent of the ER-Golgi network in these neurons (Dresbach et al., 2006; also see overlap with Golgi-marker galactosyl-transferase – GalT – below). However, we also saw BACE-1 particles (fig. 1D, arrowheads) that did not co-localize with APP, suggesting that BACE-1 may be sorted into a distinct compartment after trafficking via the ER→Golgi pathway. If the latter was true, conditions inhibiting the emergence of Golgi-derived vesicles would be expected to 'trap' APP/BACE-1 within the Golgi-network. To test this idea we incubated cultured neurons at 20°C for 2h – conditions expected to block the exit of Golgi-derived proteins (Dresbach et al., 2006). Indeed we found that the perinuclear colocalization of APP/BACE-1 was significantly increased under these conditions (fig. 1D – inset), further suggesting that the subset of somatic BACE-1 that failed to co-localize with APP at 37°C was a consequence of post-Golgi processing. Increased co-localization of BACE-1 with GalT at 20°C also supports this overall model (fig. 1D). Moreover, APP/BACE-1 colocalization decreased over 6–36 post-transfection (fig. 1D – bottom), further suggesting a differential sorting after biogenesis. The spatial segregation of APP and BACE-1 was also evident in sucrose density-gradients of P100 ("vesicle pellet", DeBoer et al., 2008 - see fractionation strategy in Supplementary fig. 1G) mouse brain fractions *in-vivo*, where endogenous holo-APP/BACE-1 were largely localized to distinct fractions (fig. 1E).

BACE-1 is largely conveyed in neuronal recycling endosomes

Next we sought to determine the specific organelles carrying BACE-1 and APP in neurons. Accordingly, we co-transfected fluorescent-tagged BACE-1 (or APP) with various labeled organelle-markers known to highlight specific biosynthetic or endosomal organelles (Yap and Winckler, 2012) and simultaneously visualized the trafficking of BACE-1/organelle-markers in dendrites by live imaging. While only ~ 10–30% of the mobile BACE-1 vesicles co-localized with Golgi markers (see below), surprisingly, the vast majority of BACE-1 was conveyed in vesicles that are known markers of neuronal recycling endosomes (fig. 2 A–C). Specifically, we simultaneously visualized transport of BACE-1:GFP and TfR:mCherry – previously used as a marker for neuronal recycling endosomes (Park et al., 2006; Wang et al., 2008). The TfR fusion construct faithfully represents a functional recycling pool, as shown in Supplementary fig. 2. Indeed the vast majority of the trafficking BACE-1 vesicles colocalized with TfR (fig. 2A–C) and also syntaxin-13 (fig. 2B – middle) – known markers of dendritic recycling endosomes (Park et al., 2006; Prekeris et al., 1999; Silverman et al., 2001; Wang et al., 2008; Yap and Winckler, 2012). In contrast, few mobile BACE-1 vesicles colocalized with Rab5, a marker for early endosomes (fig. 2B – bottom). However, unlike mobile vesicles, stationary BACE-1-cargoes colocalized with all tested markers (TfR, syntaxin 13 and Rab5 – fig. 2B). The significance of this is unclear, but such stationary particles are commonly seen when imaging vesicle transport in axons (for example, see Tang et al., 2012) and may represent sites where potential intermingling of biosynthetic and recycling organelles occur.

Next we asked if APP colocalized with known markers of the neuronal biosynthetic pathway. Towards this we co-transfected neurons with APP:mCherry and the signal-sequence of neuropeptide-Y (NPYss) fused to GFP – the latter expected to label the interior of Golgi-derived vesicles (Meskini et al., 2001; Kaech et al., 2012). Indeed the vast majority of APP vesicles colocalized with NPYss (fig. 2D **– middle**), while there was only ~ 20% colocalization of moving BACE-1 particles with NPYss (fig. 2D – right). Notably, <30% of mobile APP vesicles colocalized with TfR (27.92 ±7.0/8.33±5.45 % - mean±SEM;APP:GFP anterograde/retrograde particles respectively co-localizing with TfR:mCherry). Finally, P100 density gradients from mouse brains showed that fractions containing endogenous BACE-1 overlapped with a subset of TfR-positive vesicles; though colocalization with other

markers were variable (fig. 2E and Supplementary fig. 3). A schematic view summarizing the above data is presented in figure 2F.

Activity-induced convergence of APP and BACE-1 occurs largely in recycling compartments

The above experiments suggest that the majority of APP and BACE-1 vesicles are spatially segregated, and that APP/BACE-1 colocalization is a low frequency event under basal conditions. As physical proximity of APP and BACE -1 is an obvious requirement for initiating APP cleavage, we reasoned that conditions triggering Aβ generation (i.e. BACE-1 cleavage) should also increase APP/BACE-1 colocalization. Substantial evidence indicates that enhanced neuronal activity leads to an increase in APP cleavage and amyloidogenesis (Bero et al. 2011; Cirrito et al., 2008; Cirrito et al., 2005; Kamenetz et al., 2003, reviewed in Haass et al., 2012 – also see fig. 4D, E below). Accordingly, we first asked if induction of neuronal activity in our model-system would also increase APP/BACE-1 colocalization.

To test this idea, we transfected tagged APP and BACE-1 in cultured neurons (as above), and stimulated the neurons using established paradigms (see schematic in fig. 3A). Indeed, stimulation of neurons with glycine (Lu et al., 2001; Park et al., 2006) resulted in a significant increase in APP/BACE-1 convergence (fig. 3B, C). Pre-incubation of neurons with inhibitors of NMDA receptors prevented this colocalization (fig. 3C), indicating that these changes are a consequence of glycine/NMDA-receptor mediated pathway. Similar results were obtained when neurons were stimulated with K^+ (not shown). As an alternative approach, stimulation of neurons using the $GABA_A$ antagonist Picrotoxin (PTX) – known to increase neuronal activity in hippocampal cultures presumably due to suppression of inhibitory inputs (Neuhoff et al., 1999; Bateup et al. 2012) – also led to an increase in APP/BACE-1 convergence (fig. 3D).

What are the specific locales where APP and BACE-1 converge upon stimulation? As neuronal BACE-1 is largely localized to recycling endosomes in physiologic states (see above), we asked whether activity-induced APP/BACE-1 convergence increased APP/recycling-endosome colocalization as well. To test this hypothesis, we co-transfected neurons with APP:GFP and TfR:mCherry, and then quantified their colocalization in dendrites after stimulation with glycine and PTX in fixed neurons (see schematic in fig. 4A). Indeed a larger fraction of APP was colocalized with TfR-positive vesicles in stimulated neurons (fig. 4B). Similar experiments with APP:GFP and Rab5:mCherry (a marker for early endosomes) showed no changes in APP/Rab5 colocalization upon stimulation (fig. 4C - **left**). Similarly, BACE-1 colocalization with Rab5 was also unchanged upon activity-induction as well (fig. 4C – **right**). Treatment of neurons with a β-secretase inhibitor did not influence the activity-induced changes in the APP/BACE-1 (or APP/TfR) convergence (Supplementary fig. 4A).

The above data in fixed neurons suggest that APP and BACE-1 colocalize upon activity-induction. Next we specifically asked whether mobile APP and BACE-1 vesicles converged upon activity-induction. Towards this we co-transfected neurons with APP:GFP and BACE-1:mCh, and then stimulated them with PTX. As shown in representative kymographs (fig. 4D) and the quantification (fig. 4E), there was a striking increase in colocalization of moving APP/BACE-1 (and also APP/TfR) vesicles in the PTX-treated cells, suggesting that the mobile APP/BACE-1 particles were converging in recycling compartments upon activity-induction. Finally, stimulation of neurons led to expected increases in β-CTF generation (fig. 4F, G). Taken together, these results indicate upon neuronal activity, APP is redistributed to recycling endosomes enriched in BACE, thus facilitating β-secretase cleavage and β-CTF generation.

Activity-induced routing of APP into acidic microdomains

It has been known for some time that the aspartyl-protease BACE-1 is optimally active in an acidic pH (Vassar et al., 2009). As the intraluminal pH of recycling endosomes is also acidic (Park et al., 2006 and also see below), it is intriguing to speculate that routing of APP into acidic recycling endosomes is a key event preceding its cleavage. To test this idea directly, we used a pH-sensitive GFP (pHluorin) tagged to the N-terminus (intra-luminal end) of APP (Groemer et al., 2011) and visualized trafficking of pHl:APP in dendrites by live-imaging (see schematic in fig. 5A).

First, to test the pHluorin construct, we co-transfected neurons with pHl:APP and soluble mCherry, and monitored the fluorescence before/after lowering the pH of the media to 5.5, which would be expected to globally acidify sub-cellular compartments (Park et al., 2006). Note that the acidic pH dramatically quenches the pHl:APP but has no effect on the soluble mCherry fluorescence in the same neuron (fig. 5B), reflecting the reliability of this pH-sensitive reporter. Figure 5C shows representative kymographs of pHl:APP in dendrites before and after glycine stimulation. Note the decrease in mobile pHl:APP particles, with little change in the stationary vesicle-population (quantified in fig. 5D, left). Similar experiments with APP tagged to conventional GFP showed only a slight (non-significant) decrease in mobile vesicles after stimulation (Fig. 5D, right). Moreover we saw clear instances where the fluorescence of pHl:APP was abruptly quenched upon stimulation (see example in fig. 5E). Though such events were occasionally seen in control neurons (and we could only document them reliably in transiently-paused APP vesicles), the incidence was significantly increased upon stimulation (fig. 5E, graph and Supplementary Movie 2). Thus collectively, these experiments indicate that APP is routed into acidic compartments upon stimulation. As above, treatment of neurons with a β-secretase inhibitor did not influence the activity-induced changes in pHl-APP kinetics (Supplementary fig. 4B).

Clathrin-mediated endocytosis of APP is required for APP/BACE-1 convergence

The above data suggest that neuronal activity leads to convergence of APP vesicles with acidic recycling endosomes containing BACE-1; leading to two possible mechanistic scenarios. One possibility is that upon activity-induction, vesicles containing APP undergo endocytosis at the plasma membrane, and the endocytosed APP subsequently merges with BACE-1-positive recycling endosomes (fig. 6A, pathway [1]). Alternatively, APP/BACE-1 vesicles could undergo homotypic fusion (fig. 6A, pathway [2]). To distinguish between these two possibilities, we used the dynamin inhibitor dynasore – a drug expected to block clathrin-mediated endocytosis (CME) (Macia et al., 2006). To first characterize the effects of dynasore on CME in cultured neurons, we transfected neurons with clathrin:GFP and visualized its assembly/disassembly (“on/off”) dynamics in dendrites, known to represent coating/uncoating events inCME (Blanpied et al., 2002). Incubation with dynasore significantly increased the lifetimes of clathrin coated pits (CCPs) in dendrites (fig. 6B).

To examine the effects of endocytosis-inhibition on APP/BACE-1 colocalization, we transfected neurons with APP:GFP and BACE-1:mCherry, stimulated them with glycine in the presence or absence of dynasore, and quantified APP/BACE-1 colocalization. The main goal here was to test if inhibition of endocytosis blocked APP/BACE-1 colocalization. As shown in the representative panels (fig. 6C) and the quantification below (fig. 6D), dynasore-treatment essentially abolished the activity-dependent convergence of APP/BACE-1. However, a caveat in this experiment is that dynasore-treatment would inhibit all endocytic trafficking (not just APP) and may also suppress neuronal activity. Thus to address whether the specific inhibition of APP endocytosis would prevent its activity-induced redistribution into BACE-1-positive endosomes, we transfected neurons with APP:GFP carrying a mutation in the APP-endocytosis domain (APP-YENPTY) that is

known to inhibit APP endocytosis (Perez et al., 1999). Indeed the APP-YENPTY mutant failed to converge with BACE-1 vesicles upon stimulation (fig. 6D, image and right bar), further arguing that endocytosis of APP is specifically required for activity-dependent APP/BACE-1 convergence. Incubation of neurons with dynasore also greatly abrogated stimulation-induced increases in b-CTF's (Supplementary fig. 4C). Finally, incubation of neurons with dynasore did not alter any parameter of APP/BACE-1 transport in dendrites (Supplementary fig. 4D).

To further clarify that the stimulation-induced APP endocytosis is clathrin-dependent, we directly looked at APP and clathrin. We reasoned that if APP endocytosis was clathrin-dependent, blocking endocytosis in the setting of stimulation would inhibit the retrieval of APP from the plasma membrane and result in the stalling (and colocalization) of APP/clathrin molecules at the surface. To test this idea, we co-transfected neurons with clathrin:GFP and APP:mCherry, and simultaneously visualized both clathrin and APP fluorescence by dual-color live imaging before and after glycine stimulation (see schematic in fig. 6E). Representative kymographs from one such experiment is shown in figure 6E. Note that before adding dynasore, dynamics of clathrin and APP are largely distinct in dendrites. Expectedly, clathrin shows typical on/off kinetics while APP particles move bi-directionally. However when activity is induced in the presence of dynasore, the vast majority of clathrin and APP is colocalized (fig. 6E – right kymographs). In this setting, we also saw instances where mobile APP particles were seemingly 'captured' into stalled CCPs (fig. 6E, right). Quantification of APP movements in control and "glycine + dynasore" treated groups reveals a dramatic increase in stationary APP vesicles in the latter group (fig. 6F, left). However, there were no significant changes in BACE-1:GFP trafficking upon incubation with glycine and dynasore (fig. 6F, right). Collectively, these data further underline that the endocytosis of APP upon activity-induction is clathrin-dependent, and also suggest that the mobile fraction of APP participates in this process.

Convergence of APP and BACE-1 in Alzheimer's disease brains

Finally, we reasoned that if pathologic changes occurring in AD brains were mechanistically similar to the events suggested by our data above, one may see APP/BACE-1 convergence in AD brains as well. To test this we took a biochemical approach. P100 "membrane pellets" were obtained from 10 post-mortem frozen human AD (and control) brain homogenates, and localization of endogenous APP and BACE-1 was evaluated in sucrose density-gradients (see fractionation strategy in Supplementary fig. 1G). We found that while a spatial segregation of APP/BACE-1 was evident in age-matched control brains (fig. 7A, top – similar to mouse brains, compare with fig. 1E); in AD brains, significant amounts of APP was redistributed to higher-density fractions as well. Distribution of endogenous TfR in human brains (fig. 7A, lower panels) also overlapped with the BACE-1 fractions (similar to mouse brains – compare with fig. 2E). These data are quantified in fig. 7B, C. Note that average APP intensity in AD brains (10^{th} fraction) is significantly higher than controls (fig. 7C). Western blots showing APP distribution in all control and AD brains, as well as distribution of various organelle markers are shown in Supplementary figure 5 and 6A. Similar density-gradients from a transgenic AD mouse model (J20) also suggested a shift in APP distribution to BACE-1-enriched higher-density fractions (Supp. fig. 6B).

DISCUSSION

As both APP and BACE-1 are highly expressed in brains, and cleavage of APP by BACE-1 is the rate-limiting step in the 'amyloid pathway', an outstanding question relates to basic cellular mechanisms that limit/facilitate the convergence of APP and BACE-1 in neurons. Here we explored the dynamic localization of APP and BACE-1 using cultured hippocampal neurons as a model-system, and also validated key predictions derived from these

experiments *in-vivo*. We found that after synthesis, APP and BACE-1 are largely sorted into distinct trafficking organelles, but neuronal activity – a known trigger of amyloidogenesis – routed APP into BACE-1-containing acidic organelles via clathrin-dependent endocytosis. As BACE-1 is optimally active in an acidic pH, our experiments suggest that neurons have evolved unique trafficking strategies that limit APP/BACE-1 proximity, and we speculate that AD pathology results from the breakdown of such well-orchestrated trafficking pathways.

Spatial segregation of APP and BACE-1 in physiologic states

We found that a large fraction of vesicles carrying APP and BACE-1 are spatially segregated in neurons, both in a reduced cell-culture system (fig. 1B–D), as well as in mouse (fig. 1E) and human brains (fig. 7). Though both trans-membrane proteins are synthesized via the ER→Golgi as expected, BACE-1 is subsequently present in recycling endosomes. Though the exact steps by which this sorting occurs is unclear (true for neuronal cargoes in general, see Yap and Winckler, 2012), our data showing that BACE-1-vesicles are co-transported with several markers of recycling endosomes (fig. 2A–C) argue that BACE-1 is largely conveyed in recycling endosomes. We posit that this simple spatial separation limits APP cleavage by BACE-1 under normal conditions, perhaps leading to the low levels of Aβ physiologically detected in human brains and cerebrospinal fluid.

A pathway for activity-dependent convergence of APP and BACE-1

Substantial evidence indicates that neuronal activity triggers amyloidogenesis (reviewed in Haas et al., 2012). We found that various paradigms inducing activity in cultured neurons also led to increased colocalization of APP/BACE-1, as well as a routing of APP into recycling endosomes containing BACE-1 (fig. 3, 4), along with increased β-cleavage of APP (fig. 4F). Early studies in cell-lines suggested that APP/BACE-1 convergence occurs at or perhaps near the plasma membrane (Kinoshita et al., 2003; von Arnim et al., 2008), but more recent data (also mostly in non-neuronal cells or neuronal cell-lines) suggest that these two protein converge within early endosomes (Rajendran et al., 2006; Sannerud et al. 2011). Other studies show that APP and Rab5 may colocalize in presynaptic terminals (Ikin et al., 1996, Sabo et al., 2003). However in our experiments, mobile BACE-1 vesicles in dendrites show scant colocalization with Rab-5, a marker of early endosomes (fig. 2B, bottom). Moreover, although APP is routed to TfR-positive recycling endosomes upon glycine/PTX stimulation (fig. 4B), there is no increase in APP colocalization with Rab-5 upon activity-induction (fig. 4C).

Though these data suggest that the activity-induced convergence of APP and BACE-1 occur in neuronal recycling endosomes, we cannot exclude the possibility of a transient convergence in early endosomes as well. For example given the known dynamics of endosomes, a transitory convergence of APP/BACE-1 in early endosomes (before their appearance in recycling compartments) is conceivable. However, at the earliest times that we can image after activity-induction – typically a few minutes – APP is already present in recycling endosomes. Moreover BACE-1 is also present in recycling – and not early – endosomes, where the convergence seems to occur. Nevertheless convergence of APP and BACE-1 in early endosomes may also occur as an independent event that cannot be visualized by our methods, and/or as a transient intermediate event during APP recycling. The collective data in our study supports the model in fig. 6A, “pathway [1]”, and provides a potential starting point for further work that may more-precisely pinpoint the temporal kinetics of such convergence.

What are the specific cell-biological mechanisms that lead to activity-dependent APP/BACE-1 convergence? A recent study suggested that activity-dependent APP processing

may occur in cholesterol-rich microdomains (Sakurai et al., 2008). Worley and colleagues also recently showed that activity-induced Arc induction led to increased γ-secretase processing of APP in dendrites (Wu et al., 2012), but early mechanisms leading to the convergence of APP/BACE-1 – initiating the rate-limiting step of βcleavage – remained unclear. We found that endocytosis of APP is essential for the activity-dependent convergence of APP/BACE-1 in neurons (fig. 6). Specifically, experimental paradigms blocking clathrin-mediated endocytosis (or APP endocytosis) also abrogated APP/BACE-1 convergence (fig. 6 C, D), and such conditions led to expected stalling/clustering of APP and clathrin (fig. 6E), suggesting that a recycling-dependent pathway (as opposed to homotypic fusion) is responsible for this convergence.

What is the relevance of our findings to human disease? Studies show that amyloid plaque deposition is most conspicuous in the 'default mode network' – a circuit that is metabolically active during uni-directed mentation (Buckner et al., 2009) – leading to the hypothesis that activity-dependent amyloidogenesis may play a role in AD (Bero et al., 2011). Though our experiments do not address this directly, our finding that APP/BACE-1 convergence is exaggerated in stimulated neurons as well as AD brains is consistent with this idea. However, other studies implicate defective Aβ clearance (and not increased Aβ production) as the primary pathologic event in AD (Mawuenyega et al., 2010), and further work is needed to clarify these issues. In summary, our studies uncover novel trafficking strategies by which neurons largely restrict APP (substrate) and BACE-1 (enzyme) in distinct organelles – thus limiting Aβ biogenesis in physiologic states (figs. 1–2); define a trafficking pathway by which APP and BACE-1 converge upon induction of neuronal activity (figs. 3–6); and finally, our data from human brains (fig. 7) suggest potential relevance of these mechanisms in human disease.

MATERIALS AND METHODS

DNA constructs, antibodies and reagents

Several constructs were obtained from other laboratories as mentioned in 'acknowledgements'. The CFP/YFP tags in the BACE-1:CFP/APP:YFP constructs were replaced by GFP or mCherry, cloned in-frame, and confirmed by sequencing (see Supplementary fig. 1). The promoter in the NPYss construct (Banker lab) was swapped with CMV. The clathrin:GFP and Rab-5:mCherry constructs were obtained from Addgene (Cambridge, MA). Antibodies used for biochemistry were: APP (1565-1; Epitomics), BACE1 (MAB931; R&D), TfR (clone H68.4; Invitrogen), Tubulin (clone DM1A, Sigma), anti-pan cadherin (ab22744, Abcam), KDEL (Ab12223, Abcam), Rab11 (71-5300, Invitrogen), GM130 (610822, BD Transduction) and Rab5 (108011, Synaptic Systems). D-AP5, dynasore, picrotoxin and memantine were from Sigma and Alexa-Transferrin-488 was from Molecular probes. Beta-secretase Inhibitor II (Calbiochem) was prepared in DMSO and neurons were treated with final 0.5 μM inhibitors for 24 h.

Hippocampal cultures and transfection

Primary hippocampal neurons were obtained from postnatal (P0-P1) CD-1 mice and cells were transfected using Lipofectamine-2000 (Invitrogen) as described previously (Roy et al., 2011). Briefly, dissociated neurons were plated at a density of 50,000 cells/cm^2 in poly-D-lysine coated (1.0 mg/ml) glass-bottom culture dishes (MatTek) and maintained in Neurobasal/B27 media (Invitrogen) supplemented with 0.5 mM glutamine. All experiments examining colocalization in fixed neurons, as well as all experiments with clathrin:GFP were performed in DIV 15–18 neurons. All transport assays were performed in DIV 6–8 neurons, as thicker dendrites in older neurons precluded reliable imaging. All animal studies were carried out in accordance with University of California guidelines.

Microscopy, live cell imaging and transport data analysis

All assays were performed 4–6 h post-transfection, on low expressers, except when noted in the figures. For each group, we analyzed ~ 100–200 vesicles from 10–15 dendrites, and each experiment was repeated in at least 2–3 separate sets of cultures. Just before imaging, neurons were transferred to Hibernate-E-based 'live-imaging' at 35–37°C (Roy et al., 2011). Distal region of the primary dendrite, or the secondary dendrites (1st order branch) were selected for imaging. All time lapse movies were acquired using an Olympus IX81 inverted epifluorescence microscope with a Z-controller (IX81, Olympus), a motorized X-Y stage controller (Prior Scientific) and a fast electronic shutter (SmartShutter). Images were acquired using an ultra-fast light source (Exfo exacte) and high-performance CCD cameras (Coolsnap HQ2, Photometrics). Image acquisitions were performed using MetaMorph software (Molecular Device). Simultaneous imaging of two spectrally distinct fluorophores was performed using a "dual cam" imaging system (Photometrics), a device that splits the emission wavelengths into separate (red/green) channel. Fluorescence intensity was attenuated to 50 % to minimize photobleaching. Imaging parameters were set at 1 frame/sec, total 200 frames and 200–400 millisecond exposure with 2 × 2 camera binning, totaling to ~ 2000 s of total imaging time for each group, suitable to capture the infrequent transport events in dendrites. For transport analysis kymographs were generated in MetaMorph, and segmental tracks were traced on the kymographs using a line tool and individual lines were saved as ".rgn" file, and the resultant velocity data (distance/time) was obtained for each track as described in Tang et al., 2012. Frequencies of particle movements were calculated by dividing the number of individual particles moving in a given direction by the total number of analyzed particles in the kymograph. For co-transport assays, dual cam videos were separated using "split view" menu and kymographs were generated for each channel (red/green). Segmental tracks were traced as mentioned above and individual lines were compared manually for each pair of kymographs for one particular video. Vesicles (red/green) were considered co-transported/co-localized if the traced lines merged when kymographs were overlaid.

Colocalization analysis

Neurons were co-transfected with desired constructs, and cells were fixed after 6–12h using 4 % paraformaldehyde/4 % sucrose. Z-stack images were captured using a 100× objective with these constant imaging-parameters: 0.2 μm z-step, 400–800 ms exposure, 1 ×1 binning, and de-convolved using the "Classic Maximum Likelihood Estimation" algorithm (Huygens, Scientific Volume Imaging B.V.). De-convolved z-stacks were then subjected to a maximum intensity projection, resulting in 2-D images for processing. Subsequent processing for all images was as performed in three steps as described below. (1) Registration between images was optimized using a 2-D cross-correlation algorithm. (2) Images were thresholded. (3) Colocalization was calculated as the fraction of area overlapping between the above-threshold structures in each image. Image alignment and colocalization analysis was performed using custom algorithms written in Matlab (Mathworks). For temperature block experiments, cell were first imaged at 37°C, followed by 2 h incubation at 20°C and re-imaged.

Activity induction, drug treatments and Alexa-TfR labeling

Glycine-stimulation was performed in DIV 15–17 neurons, essentially as described by Park and Ehlers (park and ehlers 2006). Briefly, neurons were incubated at 37°C for 5 min in E4 solution containing (in mM): 124 NaCl, 2 CaCl2, 3 KCl, 10 HEPES, 10 glucose (pH 7.4). Activity was induced with E4 supplemented with 20 μM bicuculine and 200 μM glycine for 5 min, and finally in E4 with 20 μM bicuculine for 15 min before fixation and imaging. For picrotoxin (PTX) stimulation, cells were incubated in 100 μM PTX at 37°C for the desired time, and fixed. In experiments with NMDA inhibitors, neurons were either treated with 50

μM D-APV for 2 h or 10 μM memantine for 4 h, and then activation as mentioned in text. Dynasore was used at 40 μM for 30 mins at 37°C prior to activity induction and imaging. To test the pHl:APP (see fig. 5A), neurons incubated in HEPES was replaced with MES to obtain a pH of 5.5, keeping other components in the imaging buffer remaining unchanged (124 mM NaCl, 2 mM CaCl2, 3 mM KCl, 10 mM MES, 10 mM glucose, pH 5.5) as described by Park et al 2006. To label actively recycling endosomes, neurons were loaded with 50 μg/ml Alexa 488-transferrin (Invitrogen) diluted in imaging medium for 1 h at 37°C, rinsed extensively, and imaged immediately thereafter.

Biochemical analysis of mouse and AD brain tissue

Sequential isolation and density gradient centrifugation were performed to fractionate vesicular fractions as described previously (Scott et al., 2011). Briefly, brains from 4–6 week old CD-1 mice, or frontal lobe dissected from post-mortem frozen human brains (3 AD Braak V/VI and 2 controls, obtained from the AD Research Center brain bank at UCSD) were homogenized in buffer containing 20 mM HEPES, 40 mM KCl, 5 mM EDTA, 5 mM EGTA and protease inhibitor (pH 7.2). Tissue lysate was centrifuged at 1000 g for 15 min to isolate post nuclear supernatant (S1). S1 was centrifuged at 10,200 g for 20 min to obtain synaptosome-depleted fraction (S2). Finally, S2 fraction was centrifuged at 100,000 g for 1 h at 4° to isolate soluble (S100) and vesicular (P100) fraction. For floatation assays, P100 fractions were adjusted to 45 % sucrose, and bottom loaded on a 5 % – 45 % sucrose gradient and centrifuged at 160,000 g for 16 h at 4°C in a SW55-Ti rotor in an Optima L-100 ultracentrifuge (Beckman-Coulter). Ten fractions of 0.5 ml each were collected from top of the gradient column and equal volumes were used for SDS-PAGE and western blot analysis. Blots were developed by using Pierce Fast Western Blot kit ECL Substrate, visualized by using Versa Doc Imaging system (Bio-Rad) and quantified by densitometry. For ex-vivo biochemical assays to detect APP-CTFs, DIV 16–18 neurons (50,000 cells/well) were treated with 100 μM PTX in presence of 100 nM the gamma-secretase inhibitor BMS-299897 (Anderson et al., 2005). Cells were lysed in Laemmli buffer and resolved on 16 % Tricine gel.

Statistical analysis

Routine statistical analyses were performed using Prism software (Graphpad) using the Student's *t*-test for comparing two groups and one-way ANOVA for multiple groups. A p-value of < 0.05 was considered significant. For curve-fitting (fig. 1C), the Bayesian Information Criterion was used to select a second order Gaussian model for fitting of the velocity data.

Supplementary Material

Refer to Web version on PubMed Central for supplementary material.

Acknowledgments

We thank Gopal Thinakaran (University of Chicago) for the BACE-1:CFP construct, and for helpful discussions. We also thank Gary Banker (Oregon Health and Science University), Matthew Holt (Goettingen, Germany), Rytis Prekeris (University of Colorado) and Christoph Kaether (Jena, Germany) for the TfR:mCherry/NPYss:GFP, pHluorin:APP, Syntaxin-13:GFP and APP:YFP constructs respectively; and Steve Wagner (UCSD) for the gamma-secretase inhibitor BMS-299897. This work was supported by grants from the American Federation for Aging Research (AFAR) and the NIH (P50AG005131–project-2) to S.R.

References

Anderson JJ, Holtz G, Baskin PP, Turner M, Rowe B, Wang B, Kounnas MZ, Lamb BT, Barten D, Felsenstein K, et al. Reductions in beta-amyloid concentrations in vivo by the gamma-secretase

inhibitors BMS-289948 and BMS-299897. Biochem Pharmacol. 2005; 15:689–98. [PubMed: 15670587]

Bateup HS, Takasaki KT, Saulnier JL, Denefrio CL, Sabatini BL. Loss of Tsc1 in vivo impairs hippocampal mGluR-LTD and increases excitatory synaptic function. J Neurosci. 2012; 31:8862–8869. [PubMed: 21677170]

Bero AW, Yan P, Roh JH, Cirrito JR, Stewart FR, Raichle ME, Lee JM, Holtzman DM. Neuronal activity regulates the regional vulnerability to amyloid-beta deposition. Nat Neurosci. 2011; 14:750–756. [PubMed: 21532579]

Blanpied TA, Scott DB, Ehlers MD. Dynamics and regulation of clathrin coats at specialized endocytic zones of dendrites and spines. Neuron. 2002; 36:435–449. [PubMed: 12408846]

Brunholz S, Sisodia S, Lorenzo A, Deyts C, Kins S, Morfini G. Axonal transport of APP and the spatial regulation of APP cleavage and function in neuronal cells. Exp Brain Res. 2012; 217:353–64. [PubMed: 21960299]

Buckner RL, Sepulcre J, Talukdar T, Krienen FM, Liu H, Hedden T, Andrews-Hanna JR, Sperling RA, Johnson KA. Cortical hubs revealed by intrinsic functional connectivity: mapping, assessment of stability, and relation to Alzheimer's disease. J Neurosci. 2009; 29:1860–1873. [PubMed: 19211893]

Cirrito JR, Kang JE, Lee J, Stewart FR, Verges DK, Silverio LM, Bu G, Mennerick S, Holtzman DM. Endocytosis is required for synaptic activity-dependent release of amyloid-beta in vivo. Neuron. 2008; 58:42–51. [PubMed: 18400162]

Cirrito JR, Yamada KA, Finn MB, Sloviter RS, Bales KR, May PC, Schoepp DD, Paul SM, Mennerick S, Holtzman DM. Synaptic activity regulates interstitial fluid amyloid-beta levels in vivo. Neuron. 2005; 48:913–922. [PubMed: 16364896]

DeBoer SR, You Y, Szodorai A, Kaminska A, Pigino G, Nwabuisi E, Wang B, Estrada-Hernandez T, Kins S, Brady ST, Morfini G. Conventional kinesin holoenzymes are composed of heavy and light chain homodimers. Biochemistry. 2008; 47:4535–4543. [PubMed: 18361505]

Dresbach T, Torres V, Wittenmayer N, Altrock WD, Zamorano P, Zuschratter W, Nawrotzki R, Ziv NE, Garner CC, Gundelfinger ED. Assembly of active zone precursor vesicles: obligatory trafficking of presynaptic cytomatrix proteins Bassoon and Piccolo via a trans-Golgi compartment. J Biol Chem. 2006; 281:6038–6047. [PubMed: 16373352]

Ehehalt R, Keller P, Haass C, Thiele C, Simons K. Amyloidogenic processing of the Alzheimer beta-amyloid precursor protein depends on lipid rafts. J Cell Biol. 2003; 160:113–23. [PubMed: 12515826]

Greenfield JP, Tsai J, Gouras GK, Hai B, Thinakaran G, Checler F, Sisodia SS, Greengard P, Xu H. Endoplasmic reticulum and trans-Golgi network generate distinct populations of Alzheimer beta-amyloid peptides. Proc Natl Acad Sci U S A. 1999; 96:742–747. [PubMed: 9892704]

Groemer TW, Thiel CS, Holt M, Riedel D, Hua Y, Huve J, Wilhelm BG, Klingauf J. Amyloid precursor protein is trafficked and secreted via synaptic vesicles. PLoS One. 2011; 6:e18754. [PubMed: 21556148]

Haass C, Kaether C, Thinakaran G, Sisodia S. Trafficking and Proteolytic Processing of APP. Cold Spring Harb Perspect Med. 2012; 2:a006270. [PubMed: 22553493]

Ikin AF, Annaert WG, Takei K, De Camilli P, Jahn R, Greengard P, Buxbaum JD. Alzheimer amyloid protein precursor is localized in nerve terminal preparations to Rab5-containing vesicular organelles distinct from those implicated in the synaptic vesicle pathway. J Biol Chem. 1996; 13:31783–31786. [PubMed: 8943215]

Kaech S, Huang CF, Banker G. Short-term high-resolution imaging of developing hippocampal neurons in culture. Cold Spring Harb Protoc. 2012; 2012:340–343. [PubMed: 22383653]

Kamenetz F, Tomita T, Hsieh H, Seabrook G, Borchelt D, Iwatsubo T, Sisodia S, Malinow R. APP processing and synaptic function. Neuron. 2003; 37:925–937. [PubMed: 12670422]

Kinoshita A, Fukumoto H, Shah T, Whelan CM, Irizarry MC, Hyman BT. Demonstration by FRET of BACE interaction with the amyloid precursor protein at the cell surface and in early endosomes. J Cell Sci. 2003; 116:3339–3346. [PubMed: 12829747]

Lu W, Man H, Ju W, Trimble WS, MacDonald JF, Wang YT. Activation of synaptic NMDA receptors induces membrane insertion of new AMPA receptors and LTP in cultured hippocampal neurons. Neuron. 2001; 29:243–254. [PubMed: 11182095]

Macia E, Ehrlich M, Massol R, Boucrot E, Brunner C, Kirchhausen T. Dynasore, a cell-permeable inhibitor of dynamin. Dev Cell. 2006; 10:839–850. [PubMed: 16740485]

Mawuenyega KG, Sigurdson W, Ovod V, Munsell L, Kasten T, Morris JC, Yarasheski KE, Bateman RJ. Decreased clearance of CNS beta-amyloid in Alzheimer's disease. Science. 2010; 330:1774. [PubMed: 21148344]

El Meskini R, Jin L, Marx R, Bruzzaniti A, Lee J, Emeson R, Mains R. A signal sequence is sufficient for green fluorescent protein to be routed to regulated secretory granules. Endocrinology. 2001; 142:864–873. [PubMed: 11159860]

Neuhoff H, Roeper J, Schweizer M. Activity-dependent formation of perforated synapses in cultured hippocampal neurons. Eur J Neurosci. 1999; 11:4241–4250. [PubMed: 10594650]

Park M, Salgado JM, Ostroff L, Helton TD, Robinson CG, Harris KM, Ehlers MD. Plasticity-induced growth of dendritic spines by exocytic trafficking from recycling endosomes. Neuron. 2006; 52:817–830. [PubMed: 17145503]

Perez RG, Soriano S, Hayes JD, Ostaszewski B, Xia W, Selkoe DJ, Chen X, Stokin GB, Koo EH. Mutagenesis identifies new signals for beta-amyloid precursor protein endocytosis, turnover, and the generation of secreted fragments, including Abeta42. J Biol Chem. 1999; 274:18851–18856. [PubMed: 10383380]

Prekeris R, Foletti DL, Scheller RH. Dynamics of tubulovesicular recycling endosomes in hippocampal neurons. J Neurosci. 1999; 19:10324–10337. [PubMed: 10575030]

Rajendran L, Annaert W. Membrane trafficking pathways in Alzheimer's disease. Traffic. 2012; 13:759–770. [PubMed: 22269004]

Rajendran L, Honsho M, Zahn TR, Keller P, Geiger KD, Verkade P, Simons K. Alzheimer's disease beta-amyloid peptides are released in association with exosomes. Proc Natl Acad Sci U S A. 2006; 103:11172–11177. [PubMed: 16837572]

Roy S, Yang G, Tang Y, Scott DA. A simple photoactivation and image analysis module for visualizing and analyzing axonal transport with high temporal resolution. Nat Protoc. 2011; 7:62–68. [PubMed: 22179592]

Sabo SL, Ikin AF, Buxbaum JD, Greengard P. The amyloid precursor protein and its regulatory protein, FE65, in growth cones and synapses in vitro and in vivo. J Neurosci. 2003; 23:5407–5415. [PubMed: 12843239]

Sakurai T, Kaneko K, Okuno M, Wada K, Kashiyama T, Shimizu H, Akagi T, Hashikawa T, Nukina N. Membrane microdomain switching: a regulatory mechanism of amyloid precursor protein processing. J Cell Biol. 2008; 183:339–352. [PubMed: 18936252]

Sannerud R, Declerck I, Peric A, Raemaekers T, Menendez G, Zhou L, Veerle B, Coen K, Munck S, De Strooper B, et al. Proc Natl Acad Sci U S A. 2011; 108:E559–568. [PubMed: 21825135]

Scott DA, Das U, Tang Y, Roy S. Mechanistic logic underlying the axonal transport of cytosolic proteins. Neuron. 2011; 70:441–454. [PubMed: 21555071]

Silverman MA, Kaech S, Jareb M, Burack MA, Vogt L, Sonderegger P, Banker G. Sorting and directed transport of membrane proteins during development of hippocampal neurons in culture. Proc Natl Acad Sci USA. 2001; 98:7051–7057. [PubMed: 11416186]

Tang Y, Scott DA, Das U, Edland SD, Radomski K, Koo EH, Roy S. Early and selective impairments in axonal transport kinetics of synaptic cargoes induced by soluble amyloid beta-protein oligomers. Traffic. 2012; 13:681–693. [PubMed: 22309053]

Thinakaran G, Koo EH. Amyloid precursor protein trafficking, processing, and function. J Biol Chem. 2008; 283:29615–29619. [PubMed: 18650430]

Vassar R, Kovacs DM, Yan R, Wong PC. The beta-secretase enzyme BACE in health and Alzheimer's disease: regulation, cell biology, function, and therapeutic potential. J Neurosci. 2009; 29:12787–12794. [PubMed: 19828790]

von Arnim CA, von Einem B, Weber P, Wagner M, Schwanzar D, Spoelgen R, Strauss WL, Schneckenburger H. Impact of cholesterol level upon APP and BACE proximity and APP cleavage. Biochem Biophys Res Commun. 2008; 370:207–212. [PubMed: 18374657]

Wang Z, Edwards JG, Riley N, Provance DW Jr, Karcher R, Li XD, Davison IG, Ikebe M, Mercer JA, Kauer JA, Ehlers MD. Myosin Vb mobilizes recycling endosomes and AMPA receptors for postsynaptic plasticity. Cell. 2008; 135:535–548. [PubMed: 18984164]

Wei W, Nguyen LN, Kessels HW, Hagiwara H, Sisodia S, Malinow R. Amyloid beta from axons and dendrites reduces local spine number and plasticity. Nat Neurosci. 2010; 13:190–6. [PubMed: 20037574]

Wu J, Petralia RS, Kurushima H, Patel H, Jung MY, Volk L, Chowdhury S, Shepherd JD, Dehoff M, Li Y, et al. Arc/Arg3.1 regulates an endosomal pathway essential for activity-dependent beta-amyloid generation. Cell. 2012; 147:615–628. [PubMed: 22036569]

Yap CC, Winckler B. Harnessing the power of the endosome to regulate neural development. Neuron. 2012; 74:440–451. [PubMed: 22578496]

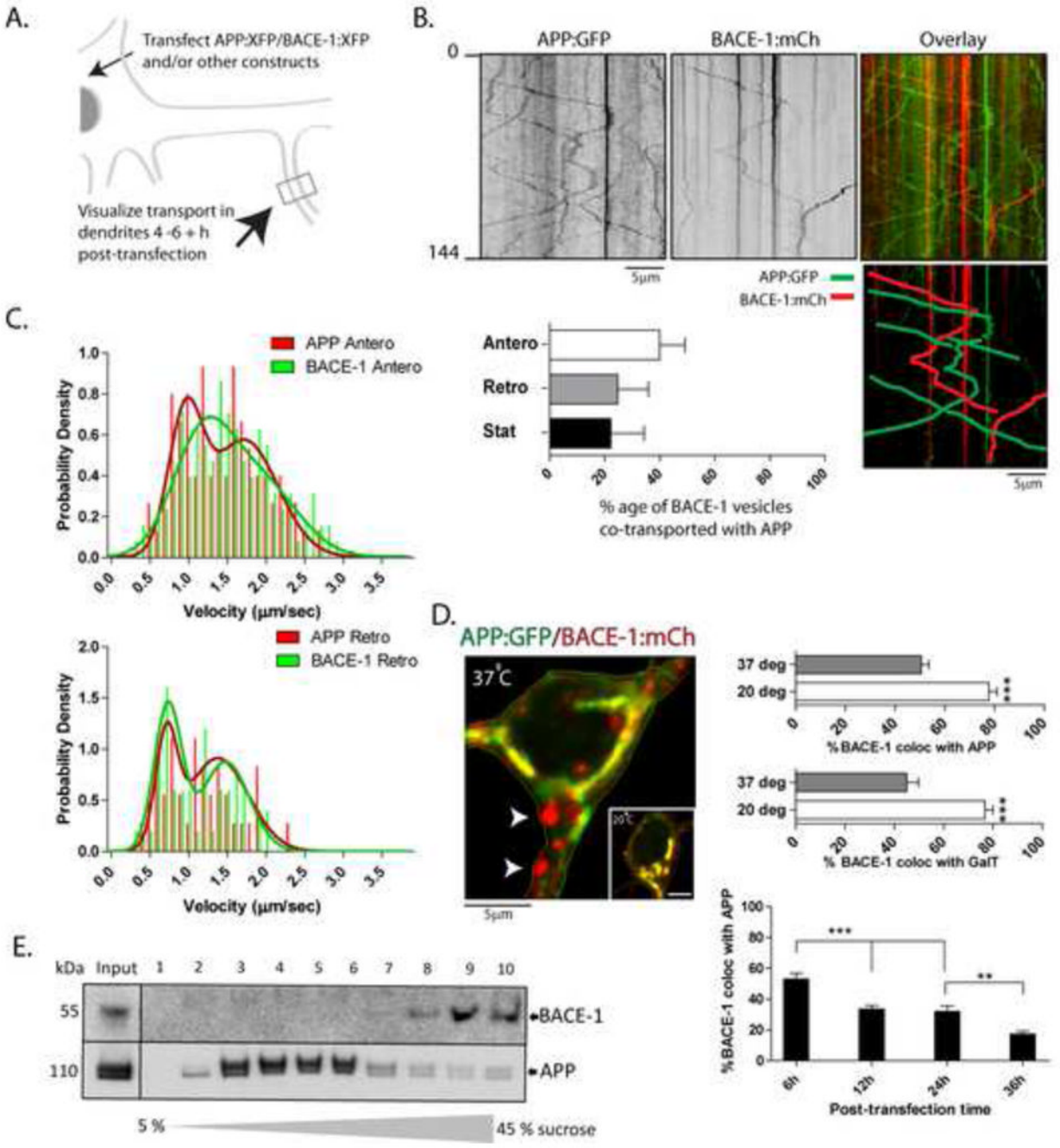

Figure 1. Segregation of APP and BACE-1 into distinct neuronal microdomains

(A) Generic plan for transport experiments. Cultured hippocampal neurons were transfected with tagged APP/BACE-1 (or other) constructs, vesicle-transport in dendrites was imaged live after 4–6 h, and resultant kymographs were analyzed (see methods for more details).

(B) Representative kymographs from simultaneous APP:GFP and BACE-1:mCherry imaging. Pseudocolor overlay of the two kymographs (top right), with mobile tracks marked (below right). Note little overlapping of mobile and stationary APP and BACE-1 vesicles, quantified in the bar-graph below.

(C) Velocity-histograms of mobile APP and BACE-1 vesicles were best-fitted by two ‘peaks’ (arrowheads – also see Tang et al., 2012), with subtle differences in anterograde

transport kinetics. The distribution of 1st and 2nd anterograde peaks for APP and BACE was significantly different (APP: 0.33/0.67; BACE: 0.5/0.5; 1st and 2nd peak respectively; p = . 0216), while distribution of 1st and 2nd retrograde peaks was not (APP: 0.29/0.71; BACE: 0.45/0.55, 1st and 2nd peak respectively; p = 0.2549).

(D) Neurons were transfected with BACE-1:mCherry and APP:GFP as above, and BACE-1/APP distribution in the soma was analyzed after 4–6h. Note that although a large fraction of the BACE-1 co-localizes with APP in a perinuclear ER→Golgi pattern, vesicles containing BACE-1 (but no APP) are also seen (arrowheads). Incubation of neurons at 20°C for 2h (expected to block exit of vesicles from the Golgi) greatly increases BACE-1/APP co-localization. Similar results were obtained with BACE-1 and GalT – a Golgi-marker. Over time, the extent of APP/BACE-1 colocalization was also diminished, further suggesting differential redistribution of these two proteins after biogenesis. n ≈ 15 neurons analysed for each temperature, from at least two separate cultures. *p < 0.05; **p < 0.01; ***p < 0.001; two tailed, unpaired *t*-test. **(E)** Sucrose density gradients from ‘vesicle-pellet’ fractions of mouse brains (see text) show that endogenous APP and BACE-1 is also largely segregated *in-vivo*.

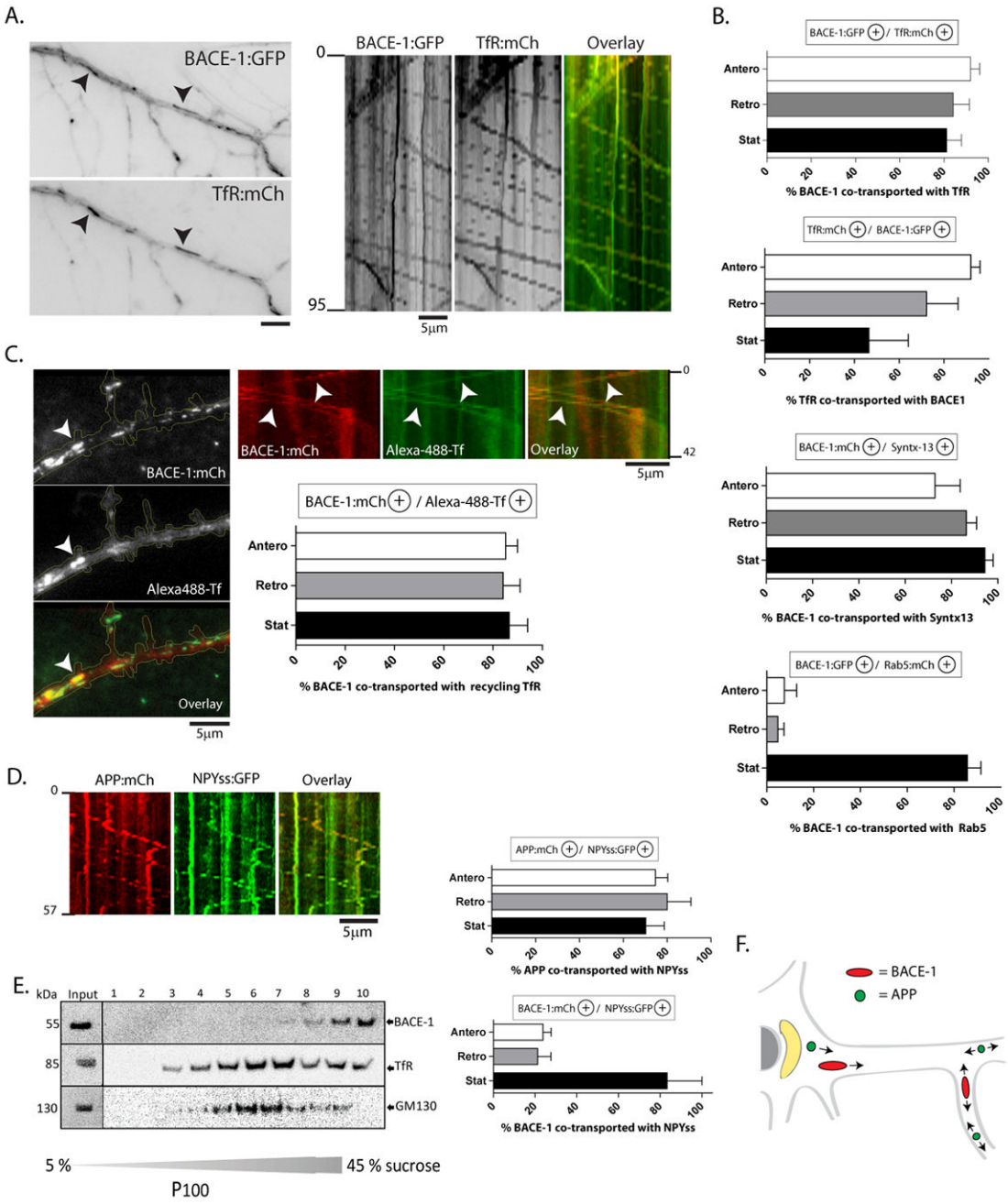

Figure 2. Trafficking of BACE-1 in recycling endosomes

(A) Neurons were co-transfected with BACE-1:GFP (or BACE-1:mCherry) and either markers of recycling endosomes (TfR:mCherry or Syntaxin-13:GFP), or a marker of early endosomes (Rab5:mCherry), and the BACE-1/endosomal organelles were simultaneously tracked by live imaging.

(B) Quantification: Note that the majority of mobile BACE-1 particles are co-transported with markers of recycling endosomes. Although BACE-1 colocalized with stationary Rab5 +ve organelles, there was little colocalization of BACE-1 with mobile Rab5. Also note that the BACE-1/TfR colocalization data suggest that BACE-1 is present in a subset of TfR+ve vesicles.

(C) Active recycling endosomes were labeled by incubating neurons with Alexa-488-Tf (see methods). These methods labeled a subset of all TfR:mCherry-positive vesicles, as expected (Supplementary fig. 2). The vast majority of Alexa-488-Tf-labeled vesicles were co-localized/co-transported (arrowheads) with BACE-1:mCherry in dendrites.
(D) A large fraction of APP (but not BACE-1) is co-transported with NPYss:mRFP – a marker expected to label the interior of Golgi-derived vesicles (Kaech et al., 2012).
(E) Sucrose density gradients from 'vesicle-pellet' fractions of mouse brains (see text) show an overlap of endogenous BACE-1 a subset of TfR-containing vesicles, but little overlap with the Golgi marker GM-130.
(F) Summary schematic. After synthesis in the ER/Golgi, BACE-1 is routed into recycling endosomes whereas APP remains in Golgi-derived vesicles, leading to a spatial segregation of these two cargoes under physiologic conditions.

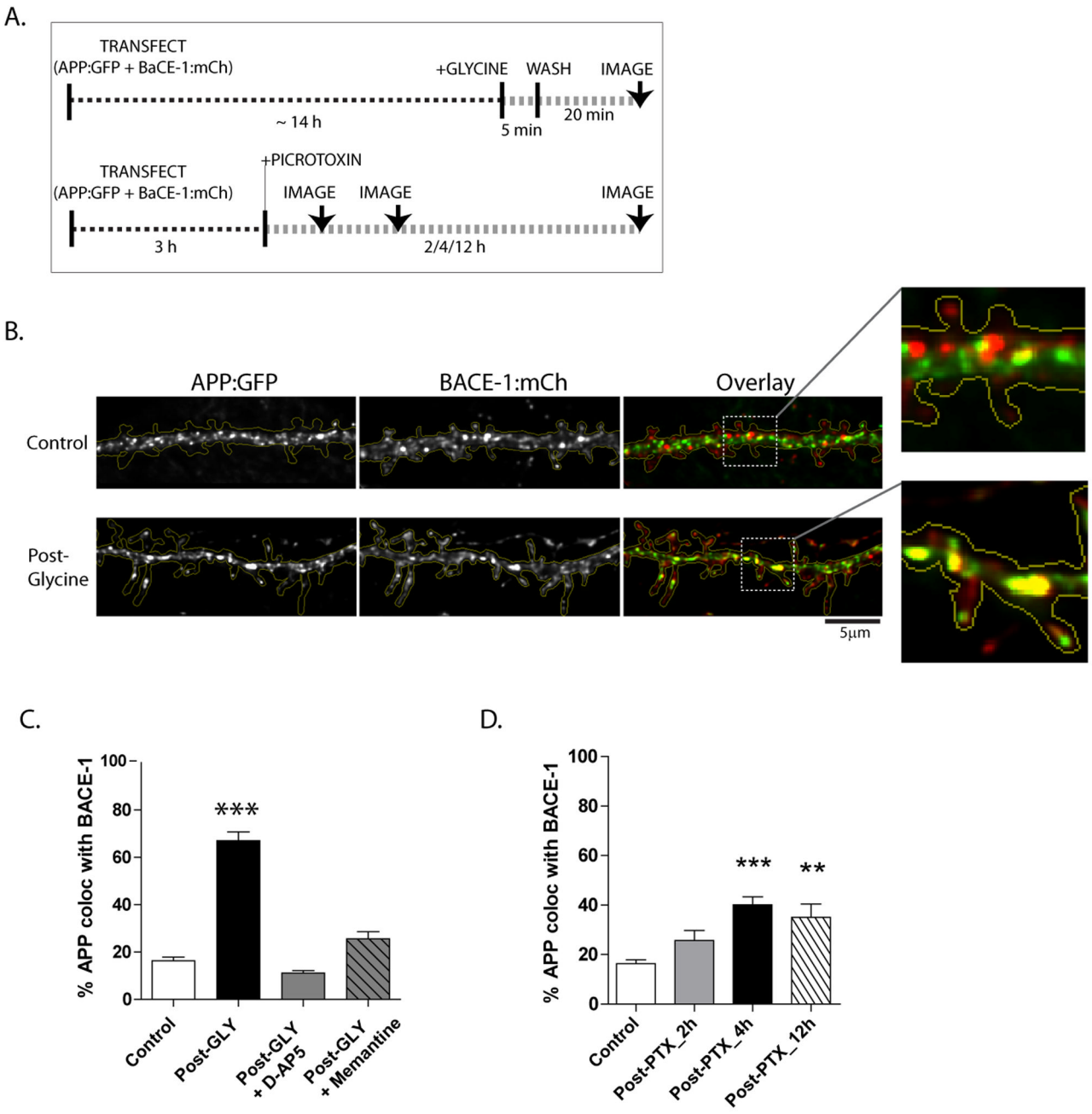

Figure 3. Activity-dependent convergence of APP and BACE-1

(A) Schematic of experiments to induce activity. Neurons were co-transfected with APP:GFP and BACE-1:mCherry, neurons were stimulated with glycine or picrotoxin (PTX), and the co-localization of APP and BACE-1 fluorescence was analyzed (see methods for more details).

(B) Note that stimulation with glycine greatly increased APP/BACE-1 colocalization in dendrites (overlaid images on right).

(C and D) Quantification of APP/BACE-1 colocalization. Note that increases in glycine-induced APP/BACE-1 convergence can be blocked by the NMDA-receptor blockers D-AP5 and memantine. n ≈ 15 neurons analysed for each condition, from at least three separate

culture sets. *p < 0.05; **p < 0.01; ***p < 0.001 compared to control by one-way ANOVA followed by Dunnet's post hoc test (C) and *p < 0.05; **p < 0.01; ***p < 0.001; two tailed, unpaired *t*-test (D).

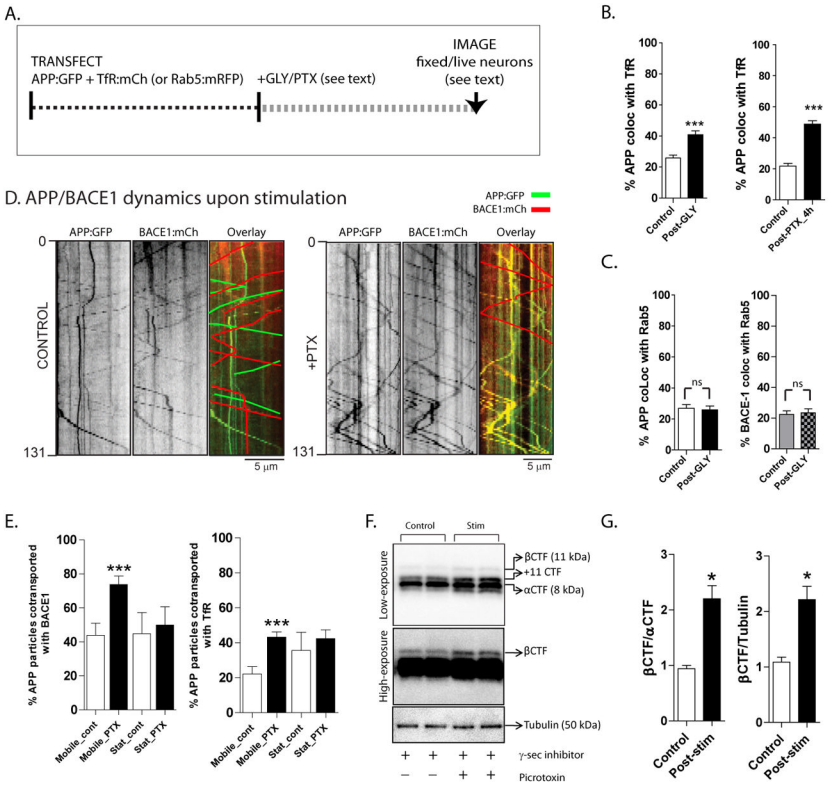

Figure 4. Routing of APP into recycling endosomes, and increased β-cleavage upon activity-induction

(A) Schematic of experiments. Neurons were co-transfected with APP:GFP and TfR:mCherry/Rab-5:mCherry to label the recycling/early endosomal compartments respectively, stimulated by glycine or picrotoxin (see methods), and colocalization of APP/TfR was analyzed in dendrites of fixed or living neurons.

(B) Note the increased colocalization of APP with TfR +ve vesicles upon stimulation.

(C) APP or BACE-1 colocalization with Rab5 was unchanged upon stimulation. For (B, C) n ≈ 20 neurons analysed for each condition, from at least three separate cultures sets. *p < 0.05; **p < 0.01; ***p < 0.001; two tailed, unpaired *t*-test.

(D) Transfected neurons were imaged before and after stimulation with PTX. While there was little convergence of moving APP and BACE-1 vesicles in control dendrites as expected (kymographs on left); significant convergence was seen upon PTX stimulation (kymographs on right). Note that to help visualization, non-colocalized diagonal tracks are highlighted in the overlaid kymographs by green/red lines.

(E) Quantification of (D). Note increased colocalization of moving (but not stationary) APP/BACE-1 upon PTX stimulation. Similar experiments with APP:GFP and TfR:mCherry showed an increased colocalization of motile APP/TfR vesicles upon PTX stimulation. n ≈ 200–300 particles analysed for each condition, from at least two separate cultures. ***p < 0.001; two tailed, unpaired *t*-test.

(F, G) Increased activity enhances the β-cleavage of APP. Cultured neurons were incubated with picrotoxin (to induce activity) and a γ-secretase inhibitor (to inhibit subsequent γ-cleavage and degradation of β C-terminal fragments – β CTF's). APP fragments were analyzed by Western blotting (see methods for more details). Note that these treatments lead to clear increases in β CTF's, quantified in **(F)** (*p < 0.05; two tailed, unpaired *t*-test).

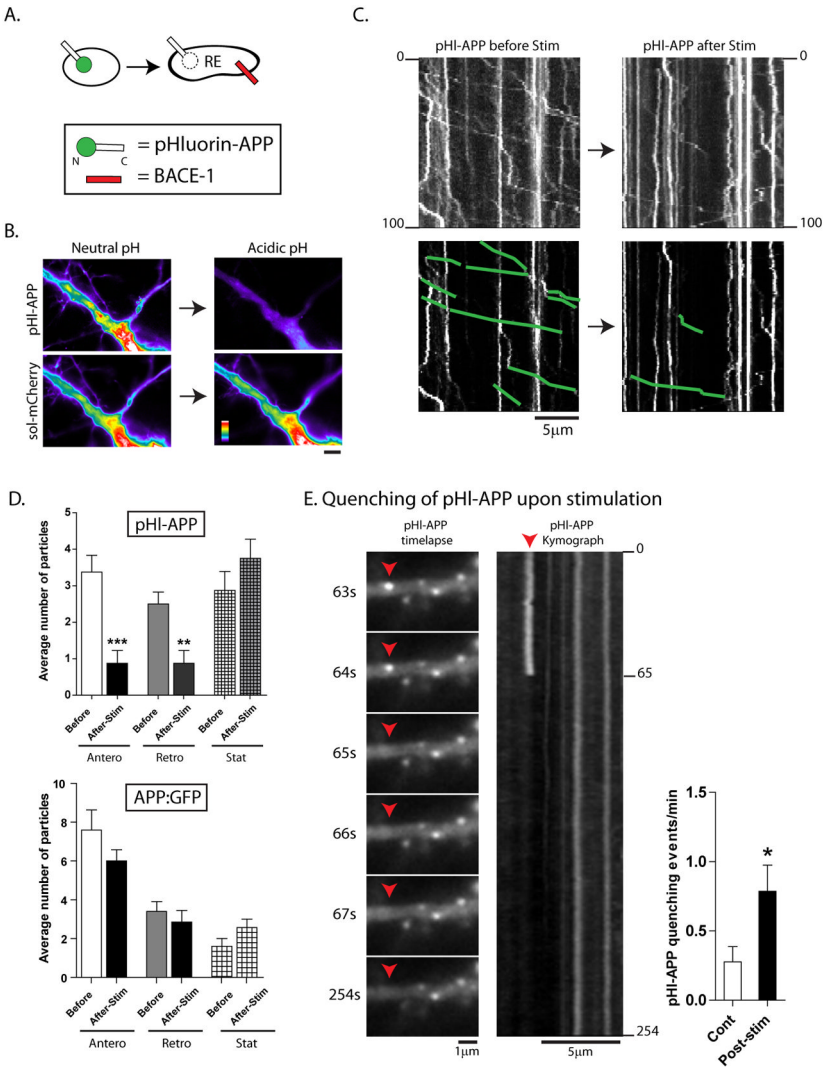

Figure 5. Mobile APP particles are routed into an acidic microenvironment upon activity-induction

(A) Schematic of pHluorin:APP. Note that the pHluorin is tagged to the N-terminus (intra-luminal) end, and would be expected to quench if APP enters into vesicles with an acidic luminal pH (i.e., recycling endosomes).

(B) To test the pHl:APP construct, neurons were co-transfected with pHl:APP and soluble mRFP, and transferred to an acidic environment (see methods). Note that while the fluorescence of the pHl:APP is dramatically quenched, there is no change in the fluorescence of soluble mRFP (all images are identically scaled, intensity 'heatmaps' shown).

(C) Neurons were transfected with pHl:APP, and vesicle-motility was analyzed – in the same dendrite – before and after stimulation. As shown in the representative kymographs (motile vesicles are traced below), though there was no change in the intensities of stationary APP particles, the number of mobile APP particles in dendrites were dramatically reduced after stimulation.

(D) Top: Quantification of motile APP particles highlight the dramatic decease upon stimulation, with little change in stationary vesicles. Bottom: Similar experiments with APP tagged to conventional GFP does not show significant decreases in mobile particles upon

stimulation. n ≈ 100–200 particles analysed for each condition, from at least two separate cultures. *p < 0.05; **p < 0.01; ***p < 0.001; two tailed, unpaired *t*-test.
(E) Upon stimulation, instances of pHl-APP quenching were also seen as shown in selected frames from a time-lapse (also see Supplementary Movie 2), further suggesting that APP was routed into an acidic compartment upon induction of neuronal activity. (*p < 0.05; two tailed, unpaired *t*-test).

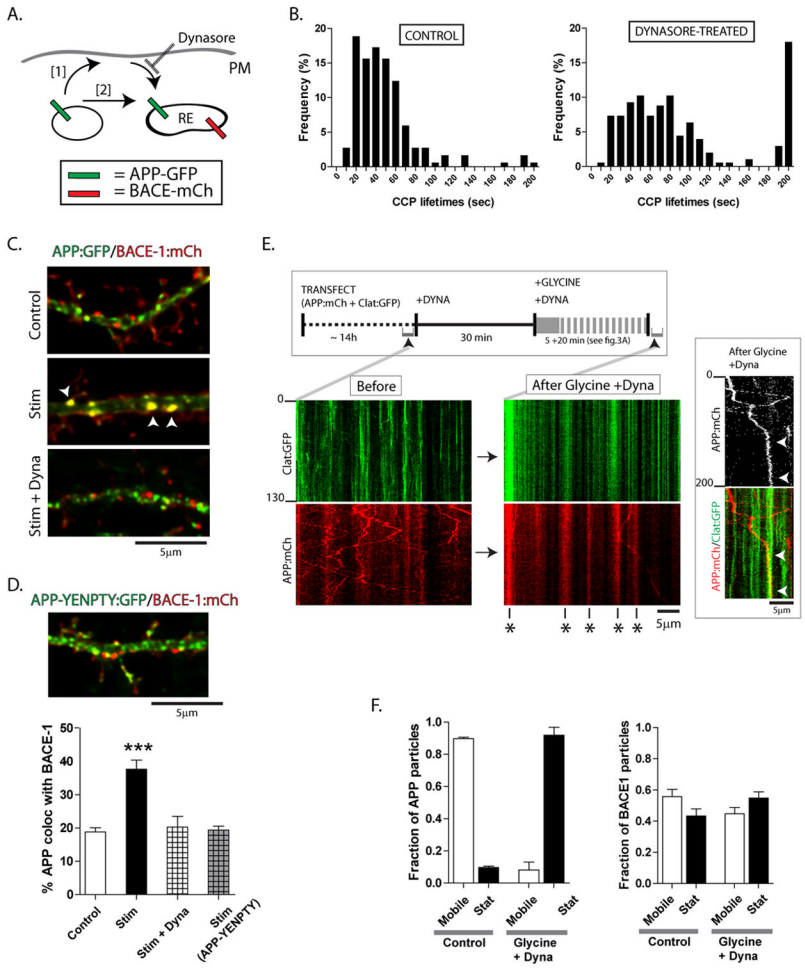

Figure 6. APP/BACE-1 convergence requires clathrin-dependent endocytosis of APP

(A) A schematic of the logic behind these experiments. The stimulation-dependent APP/BACE-1 convergence (see above) may either result after endocytosis of APP-carrying vesicles with the plasma membrane (PM), where after they mature and enter a recycling compartment (pathway [1]); or could be the result of a homotypic fusion of APP/BACE-1 carrying vesicles (pathway [2]).

(B) Upon adding dynasore – an inhibitor of dynamin – the number of clathrin coated pits (CCPs) in dendrites – as measured by on/off kinetics of clathrin:GFP – were reduced.

(C, D) Stimulation of neurons in the presence of dynasore essentially abolished APP/BACE-1 convergence. A similar inhibition of APP/BACE-1 convergence was seen using an 'endocytosis-incompetent' APP construct (YENPTY mutant, see "results"), suggesting that the abrogation of APP/BACE-1 convergence was specifically related to endocytosis of APP. n ≈ 15 neurons analysed for each condition, from at least three separate culture sets. ***p < 0.001 compared to control by one-way ANOVA followed by Dunnet's post hoc test

(E) To visualize potential APP/clathrin interactions on the dendritic surface, neurons were transfected with clathrin:GFP and APP:mCherry, and GFP/RFP mobility was simultaneously visualized before and after adding dynasore (schematic on top). Note the typical on/off events of clathrin:GFP, and bidirectional mobility of APP before adding dynasore ("before" kymographs, left). However, upon stimulation in the presence of dynasore, the vast majority of clathrin/APP particles are stationary in dendrites (stalled vesicles marked with asterisks). Inset: A motile APP particle (red) transiently pauses at sites

with stalled CCP's (green) before coming to a stop (presumably being "trapped" in a stalled CCP – arrowheads).
(F) Note dramatic increases in stationary APP particles upon dynasore + glycine treatment. Similar experiments with BACE-1:mCherry did not show significant changes in mobile fractions.

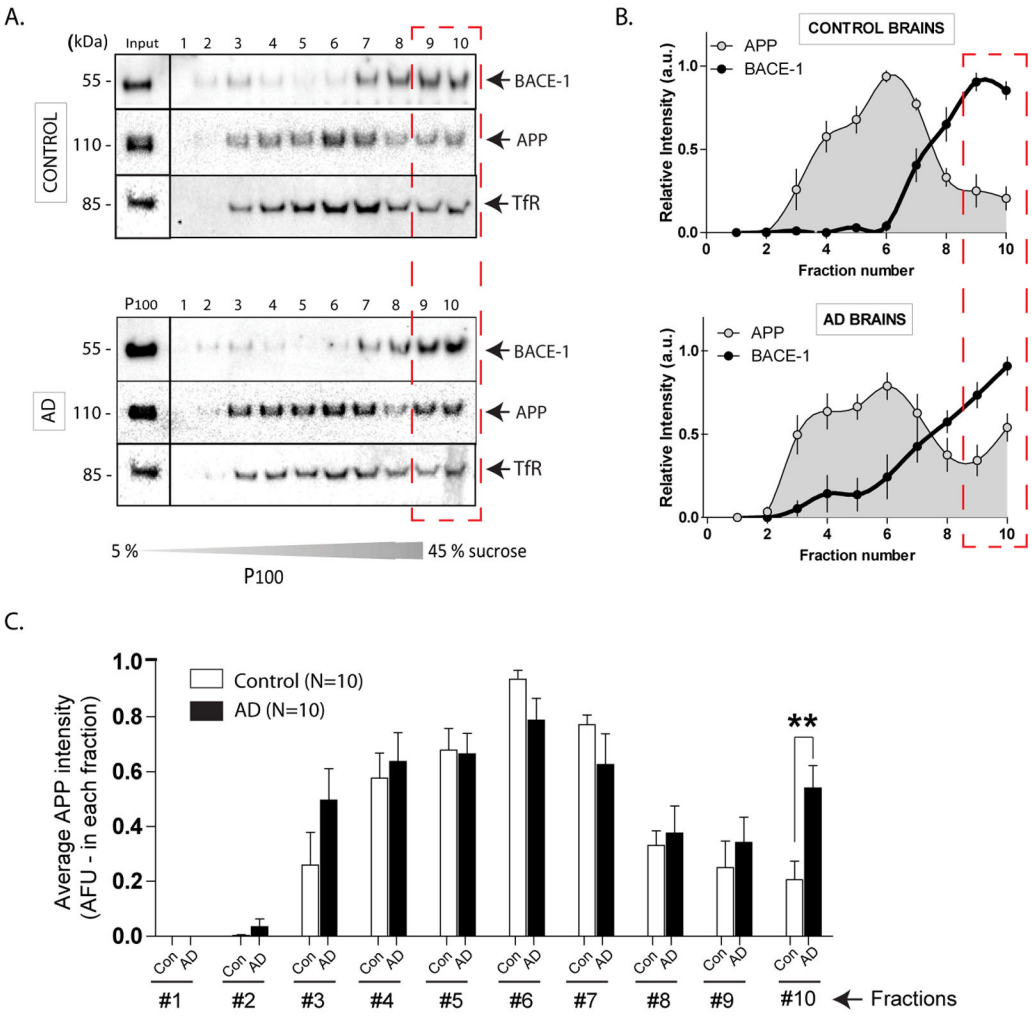

Figure 7. Endogenous APP and BACE-1 in post-mortem control and AD brains

(A) Frozen human control and AD brains were homogenized and fractionated (n=10 brains in each group, see Supplementary fig. 6). P100 “vesicle pellets” fractions were layered and separated on sucrose density-gradients and immuno-blotted with antibodies to APP and BACE-1. Similar to mouse brain homogenates (fig. 1E) endogenous APP and BACE-1 were largely localized to separate density-fractions. However, in AD brains, more APP was seen in the highest-density fractions that also contain BACE-1 (fractions 10 – hatched red box), suggesting APP/BACE-1 convergence.

(B) Densitometry analysis of the APP/BACE-1 fractions. For a given protein, the band-intensity in each lane was normalized to the maximum band-intensity of that protein over the 10 lanes. Note the relative increases in APP band-intensities in higher-density fractions from AD brains (red dashed box).

(C) Average APP blot-intensities plotted from the data shown in (B). Note the shift in APP distribution to higher-density fractions in AD brains. (*$p < 0.05$; two tailed, unpaired *t*-test).